Water content distribution in the surface layer of Maoping slope

LIU Yuewu, CHEN Huixin, LIU Qingquan, GONG Xin, ZHANG Dawei & LI Lianxiang

Division of Engineering Science, Institute of Mechanics, Chinese Academy of Sciences, Beijing 100080, China
Correspondence should be addressed to Liu Yuewu (email: lywu@imech.ac.cn)
Received July 1, 2004; accepted November 9, 2004

Abstract The water content distribution in the surface layer of Maoping slope has been studied by testing the water content at 31 control sites. The water content profiles at these sites have also been determined. The water content distributions at different segments have been obtained by using the Kriging method of geostatistics. By comparing the water content distributions with the landform of the slope, it was shown that the water content is closely dependent on the landform of the slope. The water content distribution in the surface layer provided a fundamental basis for landslide predication and treatment.

Keywords: landslide, water content, *in situ* test, Kriging method, geostatistics.

DOI: 10.1360/04zze19

1 Introduction

Pre-determination of the water content distribution of a landslide is necessary for calculating the landslide volume weight and judging the position of weak intercalary strata in the landslide. It is significant for further investigation of the landslide mechanism, the prediction of occurrence and the control of landslides[1−3]. In recent decades, remarkable advances in water content testing techniques for individual points and local average have been achieved along with considerable progress in automatic measurement techniques[4−9]. Generally, there are three kinds of water content determination methods: (i) Field point measurement methods: these methods include the direct testing method, drying weighing method, time domain reflectometery method, neutron radiation and other indirect testing methods. The advantage of the field point measurement method is that the results possess relatively high precision. The disadvantage is that either the testing sample is small or much tiresome works needs to be done to define the water content for a relatively large region. (ii) Telemetry methods: these methods can be divided into active and passive microwave measuring techniques, which include remote sensing and radar testing methods. Their advantage is that the measuring range can cover 1—1000

km^2. However, only the average water content of the whole region can be determined by these methods. (iii) Numerical simulation methods[10−13]: these methods are based on the geological and mechanical parameters of the slope layers. The methods partly depend on the test results of the above two methods, so they are only an evaluation method and do not belong to the range of field tests. There exists a range (about 0.1—10 km^2) in which it is difficult to obtain *in situ* testing results by the first and second methods mentioned above. It was indeed within this scope where numerous landslides and other geological hazards happened. How to determine the water content in this scope is one of the hot topics[14−22] in agricultural engineering, hydraulic engineering and hydrologic geology. It is also one of the issues far from being resolved, including how to deduce the water content at untested points and the space distribution of water content based on the data from the tested points.

Maoping slope was selected to assess the field test and to evaluate the method of water content distribution. Through more than two years of geological investigation and field tests, 31 test sites were selected to test the water content in the surface layers by using the drying weight and direct measurement methods. The Kriging geostatistics method and other analytical methods were employed to determine the water content distributions in the surface layer of Maoping slope based on the *in situ* tests. The water content distribution in the intermediate range has been obtained by combining the field tests and numerical analysis, and it provides the basic data for the stability analysis of Maoping landslide.

2 General geography and landform of Maoping slope

Maoping slope is located on the left bank of the Qingjiang River, 66 km above the Geheyan hydropower station and 25 km below the Shuibuya hydropower station. Maoping slope is the largest ancient landslide in the Geheyan Reservoir region, with a length of about 1600 m, a maximum width of 600 m, a thickness of 8—86 m and a total volume of about 2.350×10^7 m^3. Fig. 1 shows the profile and the geologic sketch of Maoping landslide in a birds-eye view. If the sliding body goes down at high speed, the Qingjiang River would be jammed, and the normal operation of the two hydropower stations would be affected. Additionally, Maoping slope is an ancient stack on bedrock, and this kind of slope is widely distributed within Three Gorges Reservoir region. The Geheyan Reservoir has been operating for more than ten years and its operational mode is similar to that of the Three Gorges reservoir. Hence, further study of the Maoping landslide will be valuable for the evaluation and control of landslides in the Three Gorges reservoir area.

The early investigations suggested that Maoping slope is relatively stable but that local collapse or local sliding may occur in the leading edge near the Qingjiang River after water storage. The operation of the Geheyan Reservoir began in 1993, and the maximum water level was reached in the next year. Since 1993, the deformation of Maoping slope

has been monitored by the Changjiang Water Conservancy Committee[23,24]. The monitoring data indicated that the surface deformation was very small from 1993 to 1995, but the deformation velocity subsequently increased. Up to 2001, the maximum displacement of the sliding body was 2100 mm and the annual average displacement was about 25 cm. So the abundant monitoring data is useful and very important to probe the mechanism of the initiation and evolution of the landslide.

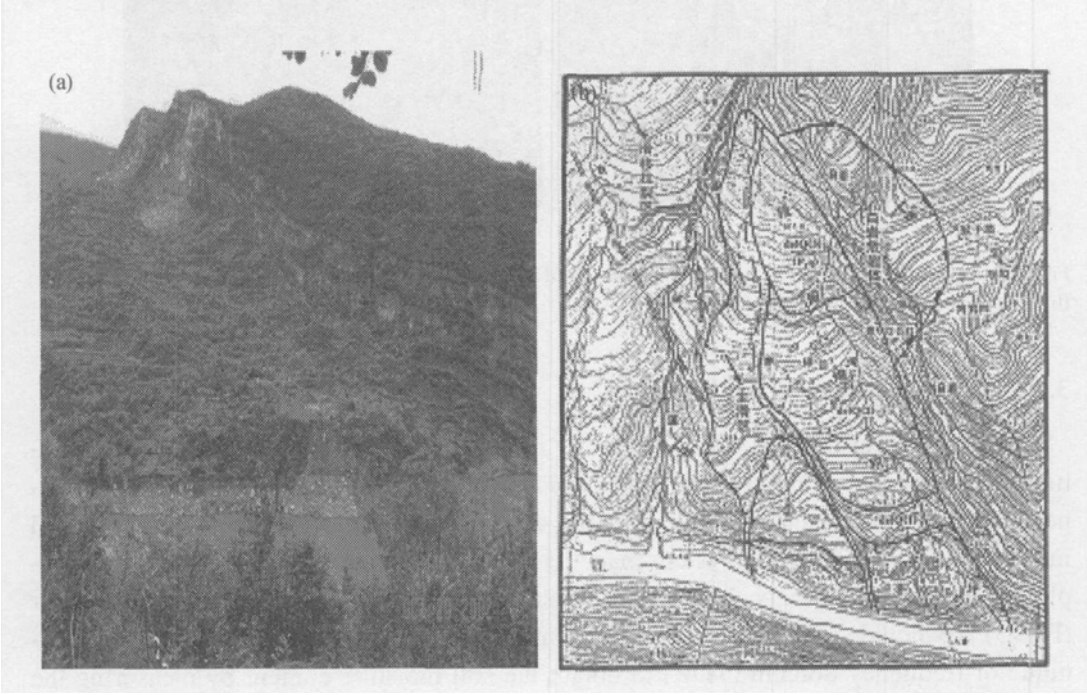

Fig. 1. Diagram of Maoping slope in the Qingjiang River. (a) Photo of Maoping slope; (b) geologic ichnograph of Maoping slope.

3 Test approach and instrument

3.1 Drying weight method

The drying weight method is widely used to measure soil water content. Its basic principle is to dry the collected soil sample in an oven and to calculate the water content by measuring the weight difference of sample before and after drying. The calculation formula is as follows:

$$\text{Water ratio } (\%) = \frac{\text{weight of wet sample} - \text{weight of dry sample}}{\text{weight of wet sample} - \text{weight of box}} \times 100\%, \qquad (1)$$

where the weight of wet sample is equal to the sum of the weight of the box and the sample weight before drying; the weight of dry sample is equal to the sum of the weight of box and the weight of the sample after drying.

The drying machine used in the experiment is DHG-9023A electric constant-tem-

perature oven (Fig. 2 (a)). The controllable temperature range is 5℃—200℃. An electric scale (made in Germany) with a precision of 0.01 g is also employed (Fig. 2 (b)).

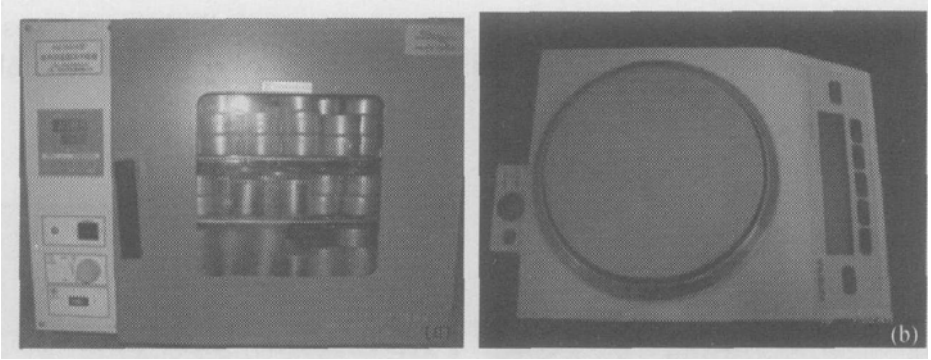

Fig. 2. Instruments used in drying weight method. (a) DHG-9023A electric constant-temperature blasting dry box; (b) electric scale with the precision of 0.01 g.

3.2 Direct measurement method

The direct measurement method directly measures the water content of the test stratum with a soil moisture tester. The measuring accuracy of the soil moisture content depends on the measuring principle and the accuracy of the tester. The thetaprobe soil moisture content measuring system made by Eijkelkamp Company of Holland was employed in the experiments. ML2x soil moisture tester and HH2 soil moisture monitor (Fig. 3) are included in this measuring system. The system employed the analytical technique of frequency domain (TDR) to obtain the soil moisture content by measuring the variation of the electric medium constant and translating it into electric voltage signals. The sensor envelope is waterproof and the four probes penetrate easily into the soil. The

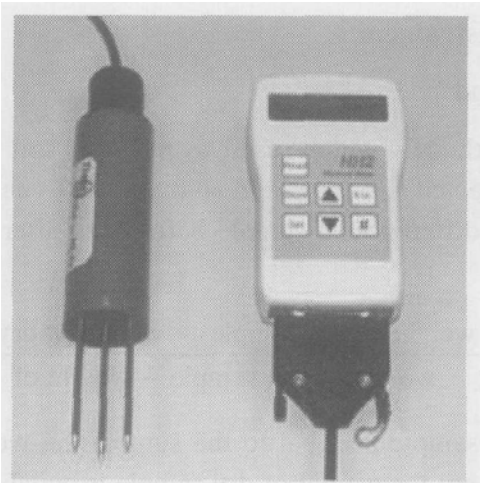

Fig. 3. Thetaprobe soil moisture measuring system.

water content range of this test system is 0%－55% and the standard calibration precision is 2%. The signal output is 0－1 V DC.

The soil moisture at the test point was measured segment by segment during the excavation process at the test sites.

4 Field test and results

4.1 Field test

Based on the survey of the geological features and the landform of Maoping slope, 31 test sites were selected scattered over the whole sliding body. Fig. 4 shows the distribution of the selected sites on the slope.

Fig. 5 is the excavated profile chart at one test site. The above-mentioned two methods were adopted to determine the soil water content at different depths throughout the excavation process. The soil samples were also taken back to the operating room. After being dried for 24 h at constant temperature (105℃), the sample was weighed and the water content of the test sample was obtained by using formula (1). Fig. 6 shows the test results of the water content profile at some test sites.

4.2 Comparison of the test results

To verify the validity of the testing system and the reliability of the test results, the test data obtained by the two different methods were compared (Table 1). The maximum relative error is about 3.343%, which is basically the same as the errors described in most references. Because the error margin is less than 3.5%, both of the methods can satisfy the engineering accuracy requirement.

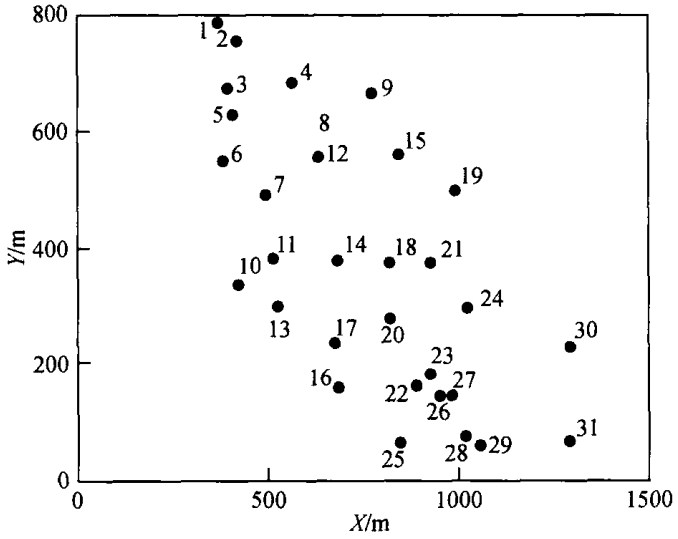

Fig. 4. Diagram of test site distribution.

Fig. 5. Excavating profile chart in one test site.

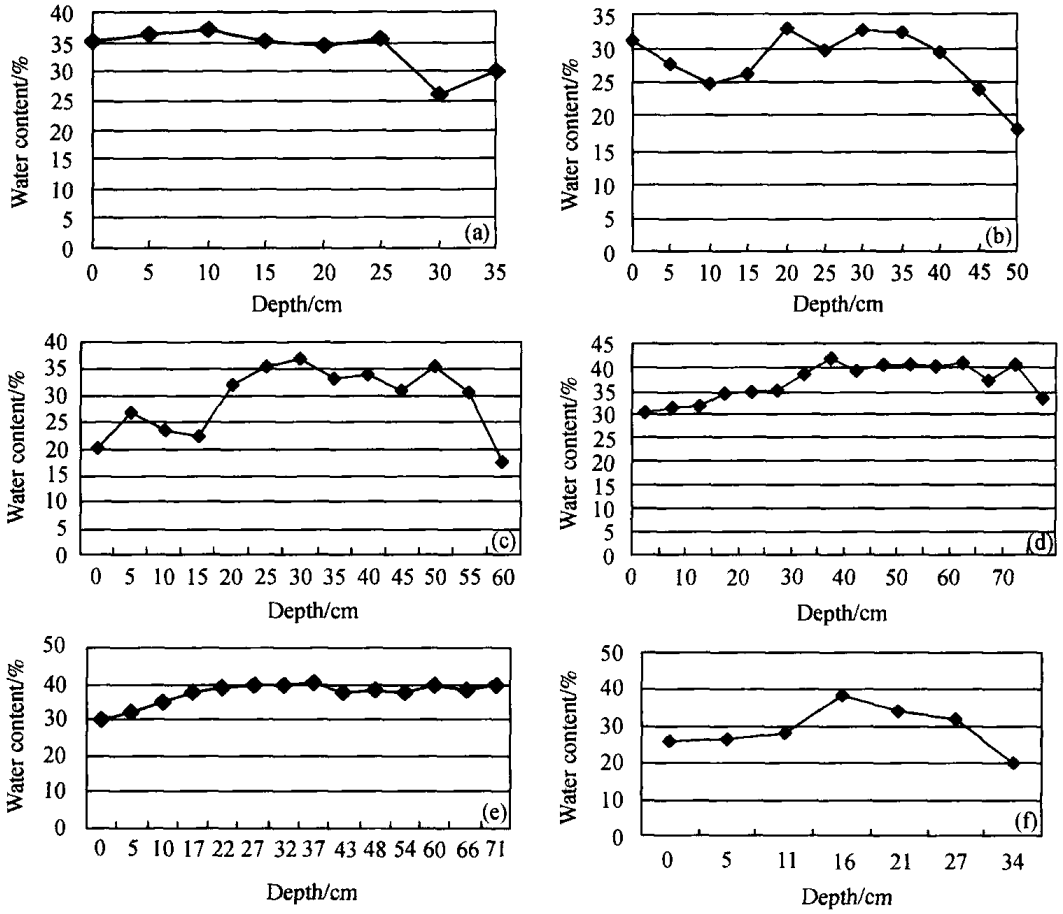

Fig. 6. Testing results of the water content profiles at some test sites. (a) Water content profile at the test site No. 9; (b) water content profile at the test site No. 26; (c) water content profile at the test site No. 23; (d) water content profile at the test site No. 13; (e) water content profile at the test site No. 25; (f) water content profile at the test site No. 19.

Table 1 Comparison of the test results by two measuring methods

Sample No.	Water content (%)		Relative error (%)	Sample No.	Water content (%)		Relative error (%)
	Drying weight method	TDR method			Drying weight method	TDR method	
1	23.1	22.8	1.299	11	27.3	26.7	2.199
2	26.1	25.9	0.769	12	27.7	27.2	1.805
3	19.5	20.1	3.077	13	27.5	27.3	0.727
4	24.4	25.2	3.277	14	20.4	20.5	0.490
5	31.6	30.8	0.633	15	32.9	31.8	3.343
6	37.2	37.1	0.269	16	34.3	33.6	2.041
7	36.6	35.9	1.926	17	37.1	36.5	1.617
8	32.3	32.1	0.619	18	34.5	34.3	0.580
9	32.4	31.9	1.543	19	35.5	34.9	1.690
10	27.2	26.8	1.471	20	37.2	36.8	1.075

5 Theoretical basis of the test data analysis

In general, only a few of the water content values can be obtained from the field test, so it is necessary to use analytical or numerical methods to evaluate the water content distribution in the whole slope. Some geo-statistical methods can be used to describe the characteristic parameters of the heterogeneous stratum. The Kriging method is one of them.

5.1 Ordinary Kriging method

Ordinary Kriging is the most widely used Kriging method. It is used to estimate a value at a point of a region for which the variogram is known, without prior knowledge of the mean. It can be used to determine the spatially distributed data by using the optimized, linear and unbiased interpolative estimation method. The method introduces the weight coefficients $\lambda_\alpha(\alpha=1,2,\cdots,n)$ for each sample to estimate the variation function. By considering the data of each sample $Z_\alpha(\alpha=1,2,\cdots,n)$ and the space structure, the geometric characteristic parameters are obtained.

The unbiased estimation condition is

$$\sum_{\alpha=1}^{n}\lambda_\alpha=1. \tag{2}$$

The estimation variance is given by

$$\sigma_E^2=\bar{C}(V,V)-2\sum_{\alpha=1}^{n}\lambda_\alpha\bar{C}(V,v_\alpha)+\sum_{\alpha=1}^{n}\sum_{\beta=1}^{n}\lambda_\alpha\lambda_\beta\bar{C}(v_\alpha,v_\beta). \tag{3}$$

That is, to evaluate the weight coefficient $\lambda_\alpha(\alpha=1,2,\cdots,n)$, the estimate variance σ_E^2 must reach a minimum value under the unbiased estimation condition.

Let $F = \sigma_E^2 - 2\mu\left(\sum_{\alpha=1}^{n}\lambda_\alpha - 1\right)$, one can get the partial derivatives vs $\lambda_\alpha(\alpha = 1,2,\cdots,n)$ and μ for F. And then, let the partial derivatives equal 0, the ordinary Kriging equations can be derived as:

$$\begin{cases} \sum_{\beta=1}^{N} \lambda_\beta \bar{C}(v_\alpha, v_\beta) - \mu = \bar{C}(v_\alpha, V), \\ \sum_{\alpha=1}^{n} \lambda_\alpha = 1, \qquad (\alpha = 1,2,...,n). \end{cases} \tag{4}$$

The estimation variance of the ordinary Kriging equation is

$$\sigma_E^2 = \bar{C}(V,V) - \sum_{\alpha=1}^{n}\lambda_\alpha \bar{C}(V, v_\alpha) + \mu. \tag{5}$$

5.2 Lognormal Kriging method

The lognormal conservation supposes that when sample values appear to follow a lognormal distribution, the sample average values follow a lognormal distribution and their combined distribution also remains a lognormal distribution. However, the linear combination of lognormal distributions disagrees with lognormal conservation.

It is suggested that the regional parameter x_α defined on the information carrier obeys the lognormal distribution, where Z is the mathematical expectation, $\bar{C}(v_\alpha, v_\alpha)$ is the variance, namely $Z = E\{x_\alpha\}$, $D^2(x_\alpha) = \bar{C}(v_\alpha, v_\alpha)$. If $y = \ln(x_\alpha)$ agrees with the normal distribution, its mathematical expectation is $Z = E\{\ln(x_\alpha)\}$, the variance is $\bar{C}_e(v_\alpha, v_\alpha) = D^2\{\ln(x_\alpha)\}$. The relationship of these two distributions is:

$$Z = \exp\left[Z_e + \frac{1}{2}\bar{C}_e(v_\alpha, v_\alpha)\right], \tag{6}$$

$$\bar{C}(v_\alpha, v_\alpha) = Z^2\left[\exp\bar{C}_e(v_\alpha, v_\alpha) - 1\right]. \tag{7}$$

When the regional parameters x_α, x_β defined on the same information carrier $v_\alpha, v_\beta(\alpha, \beta = 1,2,\cdots,n)$, obey the combined lognormal distribution with the mathematical expectation Z and the covariance $\bar{C}(v_\alpha, v_\beta)$, $\ln(x_\alpha)$ and $\ln(x_\beta)$ agree with the combined normal distribution with the covariance $\bar{C}_e(v_\alpha, v_\beta)$. Their relationship is

$$\bar{C}(v_\alpha, v_\beta) = Z^2\left[\exp\bar{C}_e(v_\alpha, v_\beta) - 1\right]. \tag{8}$$

With the lognormal Kriging method, it is suggested that if Z_V is the average value of the sample and Z_V^* indicates the evaluated value, $\ln Z_V^*$ must be the linear combination of $\ln(Z_\alpha)(\alpha = 1, 2, \cdots, n)$:

$$\ln Z_V^* = C + \sum_{\alpha=1}^{n} \lambda_\alpha \ln(x_\alpha), \tag{9}$$

where C, λ_α are the undetermined coefficients, x_α is defined on the information carrier $v_\alpha(\alpha = 1, 2, \cdots, n)$ based on the observed values of n samples.

Similar to the ordinary Kriging method, the lognormal Kriging equations are

$$\begin{cases} \sum_{\beta=1}^{n} \lambda_\beta \bar{C}_e(v_\alpha, v_\beta) - \mu = \bar{C}_e(v_\alpha, V), \\ \sum_{\alpha=1}^{n} \lambda_\alpha = 1. \end{cases} \tag{10}$$

The matrix form is $[K_e][\lambda] = [M_{2e}]$.

Eq. (10) is linear with n+1 orders. By solving the equations, weight coefficients $\lambda_\alpha(\alpha = 1, 2, \cdots, n)$ and μ can be derived. The abbreviated formula of C can be expressed as

$$C = \frac{1}{2}\left\{\sum_{\alpha=1}^{n} \lambda_\alpha \left[\bar{C}_e(v_\alpha, v_\beta) - \bar{C}_e(v_\alpha, V)\right] - \mu\right\}. \tag{11}$$

The unbiased, linear and optimized estimator Z_v^* of Z_V can be written as

$$Z_V^* = \exp\left\{\sum_{\alpha=1}^{n} \lambda_\alpha \left\{\left[\ln(x_\alpha) + \frac{1}{2}\bar{C}_e(v_\alpha, v_\alpha)\right] - \left[\frac{1}{2}\bar{C}_e(v_\alpha, V) + \frac{1}{2}\mu\right]\right\}\right\}, \tag{12}$$

where the estimated variance of Z_v^* is

$$\sigma_k^2 = Z_V^{*2}\left\{\exp \bar{C}_e(V, V) + \exp\left[\sum_{\alpha=1}^{n} \lambda_\alpha \bar{C}_e(v_\alpha, v_\alpha)\right] - 2\exp\left[\sum_{\alpha=1}^{n} \lambda_\alpha \bar{C}_e(v_\alpha, V)\right]\right\}. \tag{13}$$

6 Data analysis and discussion

The data obtained from the field test were analyzed and evaluated with both the ordinary Kriging and lognormal Kriging methods to determine the water content distribution in the surface layer of the whole Maoping slope. Fig. 7 is the water content contours in different segments of the surface layer in Maoping slope.

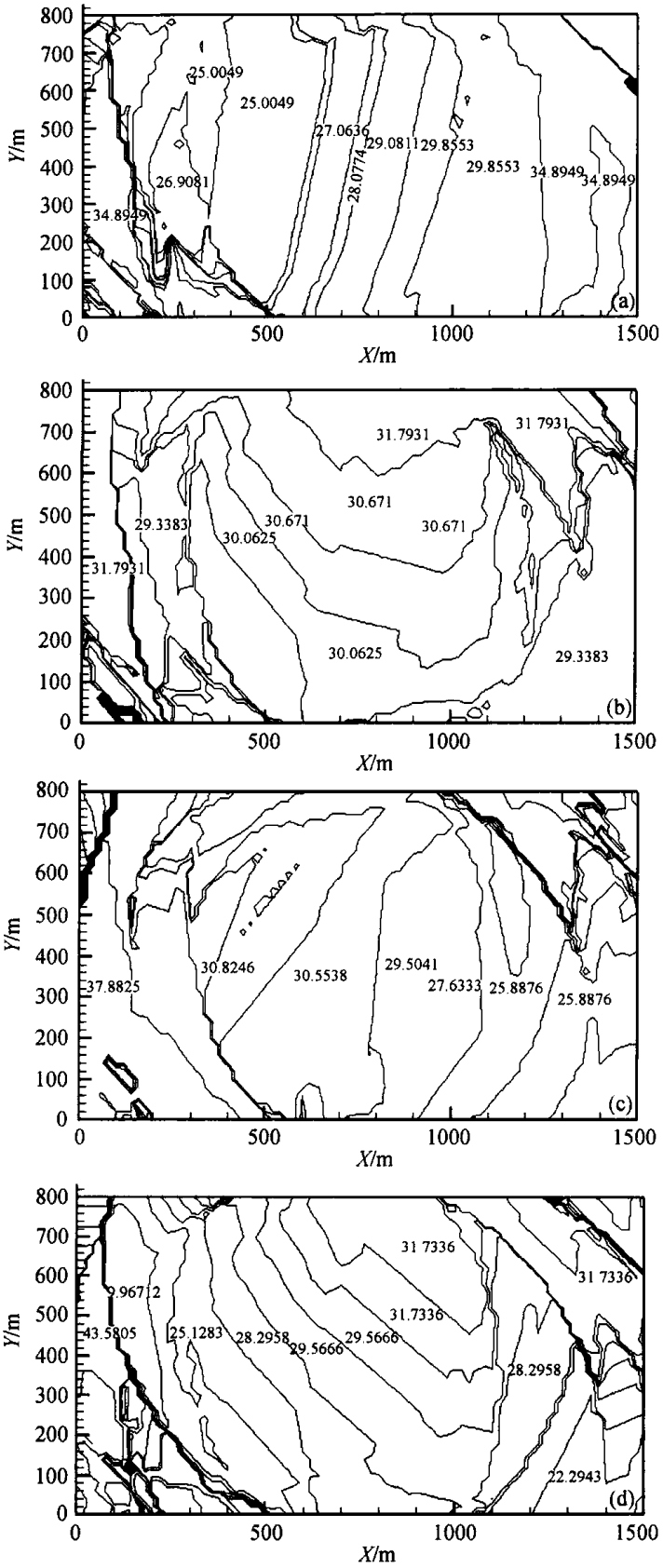

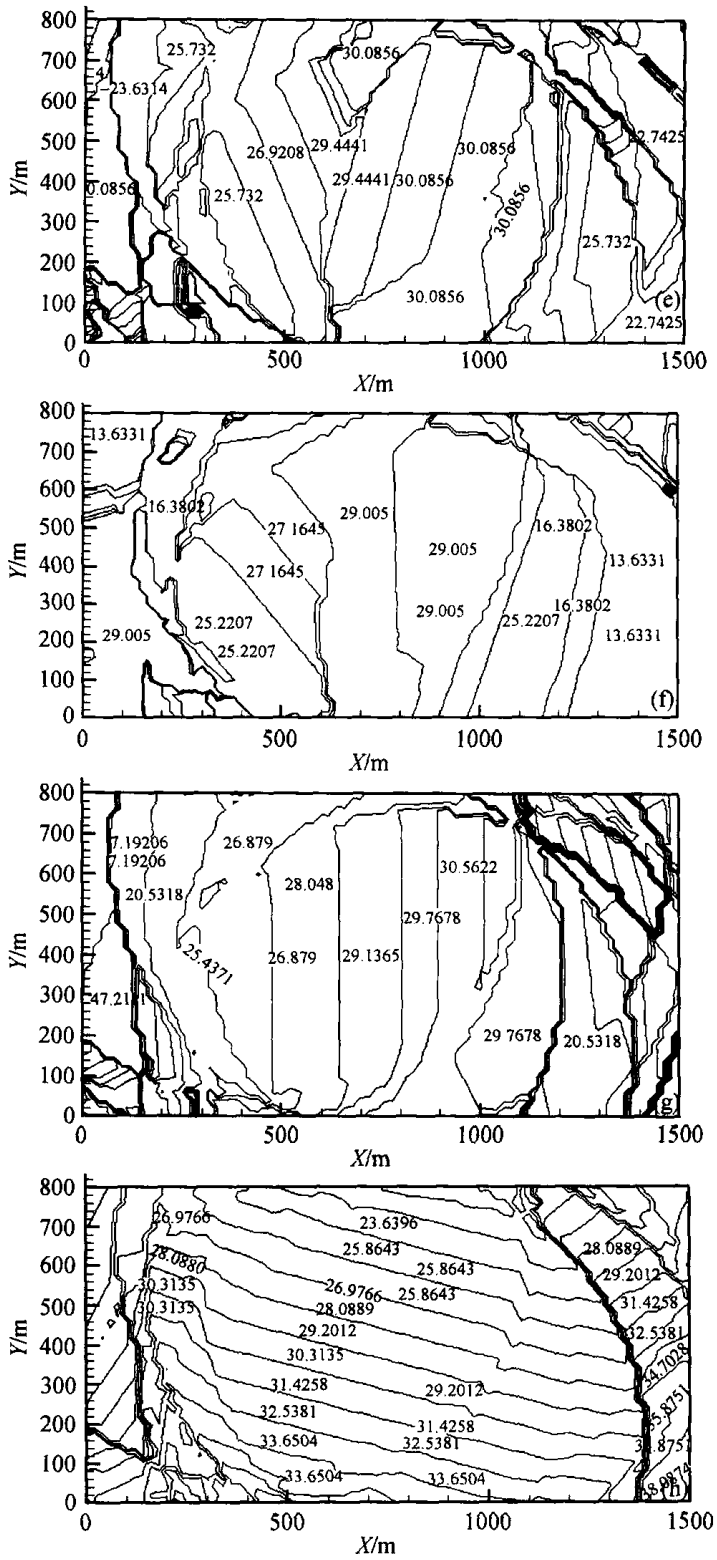

Fig. 7. Water content distribution of surface layer in different depths of Maoping slope. (a) Water content distribution at 5 cm depth; (b) water content distribution at 10 cm depth; (c) water content distribution at 15 cm depth; (d) water content distribution at 20 cm depth; (e) water content distribution at 25 cm depth; (f) water content distribution at 30 cm depth; (g) water content distribution at 35 cm depth; (h) water content distribution at 40 cm depth.

By using the Kriging method, several statistical characteristic parameters can also be obtained. These parameters are shown in Table 2. The analytical results indicated that the characteristic parameters of the water content distribution at different depths of the sliding body are normally distributed. The following conclusion can be drawn: the water content distribution is centralized and mainly at the low end of the value distribution.

Table 2 Statistic characteristic parameters evaluated with Kriging method[a)]

Layer No.	Layer deepth	Mean	Variance	Mean square derivation	C_v value	C_s value	EC value	Probability distribution type
1	00	28.156	25.207	5.021	0.178	–0.170	1.979	normal distribution
2	05	30.510	18.106	4.255	0.139	0.320	2.487	normal distribution
3	10	29.764	39.151	6.257	0.210	0.244	2.892	normal distribution
4	15	29.480	37.037	6.086	0.206	0.298	2.698	normal distribution
5	20	29.770	38.112	6.174	0.207	–0.342	2.137	normal distribution
6	25	29.027	51.268	7.160	0.247	–0.706	2.329	normal distribution
7	30	28.783	42.039	6.484	0.225	–0.531	2.213	normal distribution
8	35	28.601	37.739	6.143	0.215	–0.119	2.037	normal distribution

a) C_v is the variation coefficient, C_s is the skewness coefficient, EC is the kurtosis coefficient.

In addition, the landform map of Maoping slope (Fig. 8) shows that there exist relatively large step changes at both the top and the bottom of the landslide. The changes are basically similar to the water content step changes at the corresponding positions of the landslide, and the water content distribution changes at different depths also agree with this change. Therefore, the water content distribution in Maoping slope is in close relation with the slope landform.

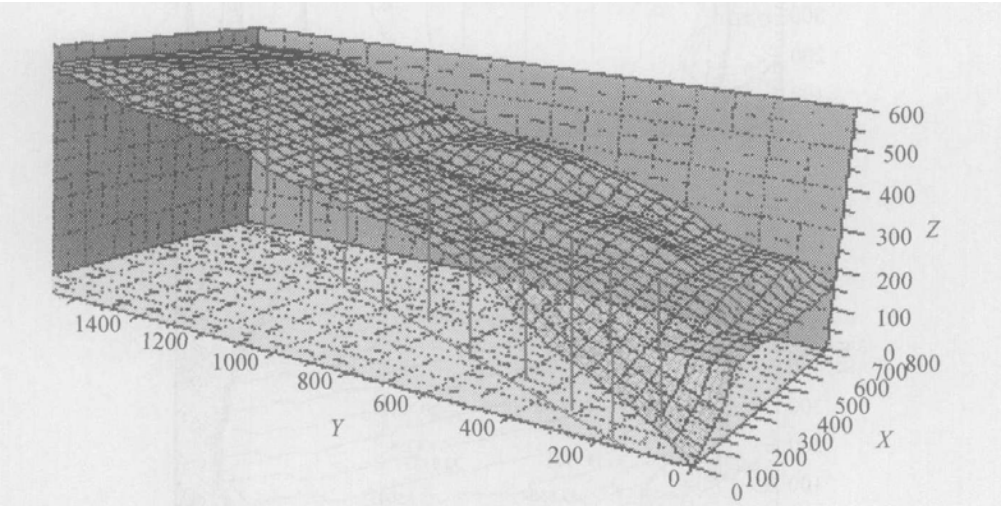

Fig. 8. Landform of Maoping slope.

7 Conclusion

Through geologic investigation and field tests, the water content profiles of the Mao-

ping landslide were obtained by using the drying weight method and the direct measurement method. On the basis of the test data, the Kriging geostatistics method was used to analyze and calculate the water content distribution of Maoping slope. The water content distribution at different depths of the slope is in close relation with the practical landform. The testing and analytical results obtained in this study provided basic data for further monitoring and treatment of Maoping landslide.

Acknowledgements The authors wish to thank all their colleagues in the Institute of Mechanics, CAS, for their valuable discussion on various parts of the work described in the paper. This work was supported by the Special Funds for Major State Basic Research Project (Grant No. 2002CB412703), the National Natural Science Foundations of China (Grant No. 10372104), and the Knowledge Innovation Project of Chinese Academy of Sciences (Grant No. KJCX2-SW-L1-4).

References

1. van den Elsen, E., Xie, Y., Liu, B. et al., Intensive water content and discharge measurement system in a hillslope gully in China, Catena, 2003, 54: 93－115.
2. Lim, T. T., Rahardjo, H., Chang, M. F. et al., Effect of rainfall on matric suctions in a residual soil slope. Canadian Geotechnical Journal, 1996, 33: 618－628.
3. Krahn, J., Fredlund, D. G., Klassen, M. J., Effect of soil suction on slope stability at Notch Hill, Canadian Geotechnical Journal, 1989, 26: 269－278.
4. Walker, J. P., Willgoose, G. R., Kalma, J. D., *In situ* measurement of soil moisture: a comparison of techniques, Journal of Hydrology, 2004, 293(1-4): 85－99.
5. Rothe, A., Weis, W., Kreutzer, K.et al., Changes in soil structure caused by the installation of time domain reflectometry probes and their influence on the measurement of soil moisture. Water Resour. Res. 1997, 33 (7): 1585－1593.
6. Topp, G. C., State of the art of measuring soil water content, Hydrol. Process, 2003, 17: 2993－2996.
7. Wilson, R. G., Methods of Measuring Soil Moisture. Technical Manual Series, Ottawa, 1971.
8. Schmugge, T. J., Jackson, T. J., McKim, H. L., Survey of methods for soil moisture determination, Water Resour. Res., 1980, 16(6): 961－979.
9. Huisman, J. A., Sperl, C. et al., Soil water content measurements at different scales: accuracy of time domain reflectometry and ground-penetrating radar, Journal of Hydrology, 2001, 245(1-4): 48－58.
10. Panigrahi, B., Panda, S. N., Field test of a soil water balance simulation model, Agricultural Water Management, 2003, 58: 223－240.
11. Walker, J. P., Willgoose, G. R., Kalma, J. D., One dimensional soil moisture profile retrieval by assimilation of near surface measurements: a simplified soil moisture model and field application, J. Hydromet., 2001, 2: 356－373.
12. van Genuchten, M. T., A closed-form equation for predicting the hydraulic conductivity of unsaturated soils, Soil Sci. Soc. Am. J., 1980, 44: 892－898.
13. Knight, J. H., Ferre, P. A., Rudolph, D. L. et al., A Numerical analysis of the effects of coatings and gaps upon relative dielectric permittivity measurement with time domain reflectometry, Water Resour. Res., 1997, 33 (6): 1455－1460.
14. Western A.W., Sen-Lin Zhou et al, Spatial correlation of soil moisture in small catchments and its relationship to dominant spatial hydrological processes, Journal of Hydrology, 2004,286(1-4): 113－134
15. Wilson, D. J., Western, A. W. Grayson, R. B. et al., Spatial distribution of soil moisture over 6 and 30 cm depth, Mahurangi river catchment, New Zealand, Journal of Hydrology, 2003, 276(1-4): 254－274.
16. Snepvangers, J. J. J. C., Heuvelink, G. B. M., Huisman, J. A., Soil water content interpolation using spatio-temporal kriging with external drift, Geoderma, 2003, 112(3-4): 253－271.

17. Schume, H., Jost, G., Katzensteiner, K., Spatio-temporal analysis of the soil water content in a mixed Norway spruce (Picea abies (L.) Karst.)-European beech (Fagus sylvatica L.) stand, Geoderma, 2003, 112(3-4): 273－287.
18. Bruckner, A., Kandeler, E., Kampichler, C., Plot-scale spatial patterns of soil water content, pH, substrate-induced respiration and N mineralization in a temperate coniferous forest, Geoderma, 1999, 93(3-4): 207－223.
19. Western, A.W., Blöschl, G., On the spatial scaling of soil moisture, Journal of Hydrology, 1999, 217(3-4): 203－224.
20. Grayson, R. B., Western, A. W., Towards areal estimation of soil water content from point measurements: time and space stability of mean response, Journal of Hydrology, 1998, 207(1-2): 68－82.
21. Western, A. W., Blöschl, G. et al., Geostatistical characterizations of soil moisture patterns in the Tarrawarra catchment, Journal of Hydrology, 1998, 205(1-2): 20－37.
22. Pelletier, J. D., Malamud, B. D., Blodgett, T. D. et al., Scale-invariance of soil moisture variability and its implications for the frequency-size distribution of landslides, Engineering Geology, 1997, 48: 255－268.
23. Ma Shuishan, Li Di, The displacement characteristics and prediction of its trend of Maoping landslip mass, Journal of Yangze River Scientific Research Institute (in Chinese), 1994, 11(3): 72－79.
24. Wang Shangqing, Yi Qinglin, The synthetic analysis on deformation characteristics and influential factors of Maoping landslide, Qingjiang, Chinese Journal of Geological Hazard and Control (in Chinese), 1999, 10(2): 40－44.